Hindawi
Geofluids
Volume 2022, Article ID 8288408, 10 pages
https://doi.org/10.1155/2022/8288408

Research Article

Study on Granite Permeability Zoning Based on Electrical Resistivity: Take Wuyue Pumped Storage Power Station as an Example

Zhiquan Huang,[1,2] Tao Ran,[2] Jinyu Dong,[2] Guangxiang Yuan,[2] and Guizhang Zhao[2]

[1]*School of Civil Engineering, Luoyang Institute of Science and Technology, Luoyang 471000, China*
[2]*College of Geosciences and Engineering, North China University of Water Resources and Electric Power, Zhengzhou 450046, China*

Correspondence should be addressed to Jinyu Dong; dongjy0552@126.com

Received 17 June 2022; Accepted 24 August 2022; Published 5 October 2022

Academic Editor: Yu Wang

A granite mass in Xinyang, China, was studied to better understand the features of the link between permeability and resistivity. The permeability coefficient of subsurface media has a certain correlation with electrical conductivity. The following steps are conducted in this method; first, water pressure tests were conducted on the borehole to determine the permeability of the granite mass at different depths; next, the electrical resistivity values of the borehole rock were determined using geophysical logging techniques; finally, three mathematical models were chosen to construct the relationship between the two, and their applicability in the study area was confirmed. The method has some applicability and can serve as a guide for the design of reservoir impermeability. It was discovered that the calibration permeability obtained by inverting the power function model has the greatest applicability and can be applied to the permeability zoning of two high-density logging lines to obtain the characteristic dividing line of 0.5 Lu and 1.0 Lu more clearly and that this method has certain applicability and can serve as a reference for the design of reservoir impermeability.

1. Introduction

By the end of 2018, China had created approximately 10,000 reservoirs, with a total reservoir capacity of 8.95×10^{11} m^3 [1]. This development has had a significant positive impact on industry, agriculture, and people's quality of life. However, reservoir leakage has been a common calamity that occurs, and leakage is caused by a number of factors. As time passes, the presence of potential leakage threats and their ongoing growth may have severe impacts on the entire reservoir dam region, further compromising the integrity of the subterranean rock structure [2, 3]. Since the 1960s in China, pumped storage power plant facilities have been investigated and researched for their significant role in regulating the peaks and troughs of electricity consumption. Today, half a century later, these facilities have made a qualitative leap in terms of installed capacity and key technologies and have spread this technology around the world to the acclaim of owners. It is common in the construction of upper reservoirs for pumped storage power plants to come across a single ridge, which is crucial to the storage efficiency and overall stability of the upper reservoir. For this reason, it is especially crucial to investigate the rock permeability and structure of the single ridge.

According to Yuan and Zhang [4], the main index for measuring the permeability of rock mass is the rock permeability coefficient obtained by water pressure tests. However, borehole methods are expensive and time-consuming, and indoor tests are affected by spatial and temporal factors, making it difficult to measure regional rock permeability accurately most of the time.

After applying an artificial current field using an array of exploration, the high-density electrical resistivity tomography method (ERT), which is noninvasive, nondestructive, quick, and cost-effective, uses the principle of different medium conductivity to obtain the distribution characteristics of the conduction current of the subsurface medium and reflects the

information about the subsurface medium through the electrical resistivity difference [4]. Through extensive data analysis, Archie created a model for the relationship between electrical resistivity and porosity of saturated cohesive soils as early as 1942. Subsequently, research on the medium resistivity theory advanced quickly [5]. Some achievements have been made in the application of electrical resistivity, such as based on special soil electrical resistivity evaluation models, based on modern multivariate electrical resistivity models, and based on temperature correction and clay conductivity correction electrical resistivity models and other models emerged in large numbers [6–18]. A new direction and advancement have been made in the use of the electrical resistivity method to obtain hydrogeological parameters as a result of the development of numerous electrical resistivity models, which are closely related to the pore water of geotechnical masses filled with electrolyte properties. Using the acquired electrical bathymetry data, Xue proposed a model for the link between hydraulic conductivity and lateral electrical resistivity of sand and pebble strata in the Chengdu Plain [19]. By analyzing the geological information of water sources outside the eastern suburbs of Nanjing, Yu and Xia built a model for the relationship between permeability and electrical resistivity of aquifers in karst environments, which was used to assess the regional hydrogeological conditions [20]. Yu and Wu used resistivity data from sandy aquifers to conduct a preliminary examination into the relationship between electrical resistivity and permeability coefficient from the similarity of current field and seepage field [21]. In alluvial aquifers in various locations, Tizro et al. and Perdomo et al., respectively, developed the correlation function between electrical resistivity and permeability. Electrical resistivity is undoubtedly a useful indication for revealing the distribution of permeability in a geotechnical material [22, 23]. There are currently few research on the relationship between the two for granites with dense structures, little water absorption, and high hardness.

The study object for this essay is a granite mass located in the Chinese City of Xinyang. In order to match the permeability coefficient data of the rock mass acquired from the water pressure test to the relational model, the electrical resistivity data at the borehole location must first be extracted. After that, the validity and applicability of the mathematical model are examined. In order to examine the spatial distribution pattern of the permeability of the granite mass and to generate new methodologies and concepts for the zoning of permeability, the electrical resistivity data from the borehole location are merged with the data.

2. Study Area and Methods

2.1. Study Area. The study location is situated in China's Xinyang City's Yinpeng Town, Guangshan County. It is a transitional zone between the North China Plain and the northern foot of the middle Dabie Mountain and is a part of the Pan Xindian-Yanjiahe hilly region. The research area's overall terrain is low in the north and high in the south, as well as low in the west and high in the east. The inner and outer slopes of the reservoir region have topographic slopes that range from 21° to 46°, with local granite escarpments. Three significant bases were created by the granite ($\gamma^5_{3\text{-}1}$) that was first intruded in the Late Yanshanian, along with a few additional smaller granite strains that were dispersed throughout the rock mass. The Laoshan granite mass in the study area is a little granite strain with grayish white, flesh red medium-grained diorite, hard and compact, and local development of grayish white fine-grained granite and quartz veins. In the thin Fenshuiling distribution region, two boreholes have been drilled, and the results show that the bottom limits of totally decomposed, severely weathered, and medium weathered rock are 2~6 m, 36.4 m, and 75 m, respectively. The location of the study region is depicted in Figure 1, where the deeper ones are typically dense joints or fractured portions of faults, as well as local cystic worn by tectonic activity.

2.2. Study Methods

2.2.1. Measurement of Electrical Resistivity. According to what was previously mentioned, the high-density electrical resistivity tomography method is based on the variation in medium conductivity. It reflects the pertinent physical characteristics of the medium (such as electrical resistivity distribution characteristics) by measuring the electrical resistivity of the medium within the range of electrode placement, and the results are then displayed as images. The field data acquisition system and the data processing system, also known as real-time processing system, make up the exploration system of ERT. In this investigation, the 200 V DC power supply, a pulse width of 0.5 s, a period of 1.0 s, and a Wenner-Alpha method for the electrode layout of the measuring line are all employed using the DUK-2B measurement system created by Chongqing Geological Instruments Co., Ltd. The measurement is performed using a symmetrical quadrupole apparatus. 19 layers are the greatest isolation factor. This time, the measurement lines were set up in two borehole locations with the intention of testing the spatial variation law of granite mass electrical resistivity at the measurement lines. The chosen instruments are shown in Figure 2, and the distribution diagram of Wenner-Alpha method measurement points is shown in Figure 3.

2.2.2. Permeability of Rock Mass. The water pressure test is a standard in situ method for determining the permeability of a rock mass, with the Lugeon water pressure test method being the most prevalent internationally. With reference to the conventional water pressure test of boreholes in the "Specification for Water Pressure Test in Borehole of Hydropower Projects" [24], a pressure gauge installed on the inlet pipe was used to measure the pressure in this study. The device's schematic diagram is depicted in Figure 4. Due to the operating concept of the drilling equipment with its own pressure machine, the conventional approach cannot eradicate backwater's influence. In order to reduce the error, an improved pressure gauge was employed in this study; specifically, a check valve was added to the entrance of the pressure gauge in order to eliminate the interference caused by pressure instability on the results [25]. In Figure 5, the field operation is depicted.

After drilling one section and inspecting one section, the top-down segmental pressure water method with 5.0 m as

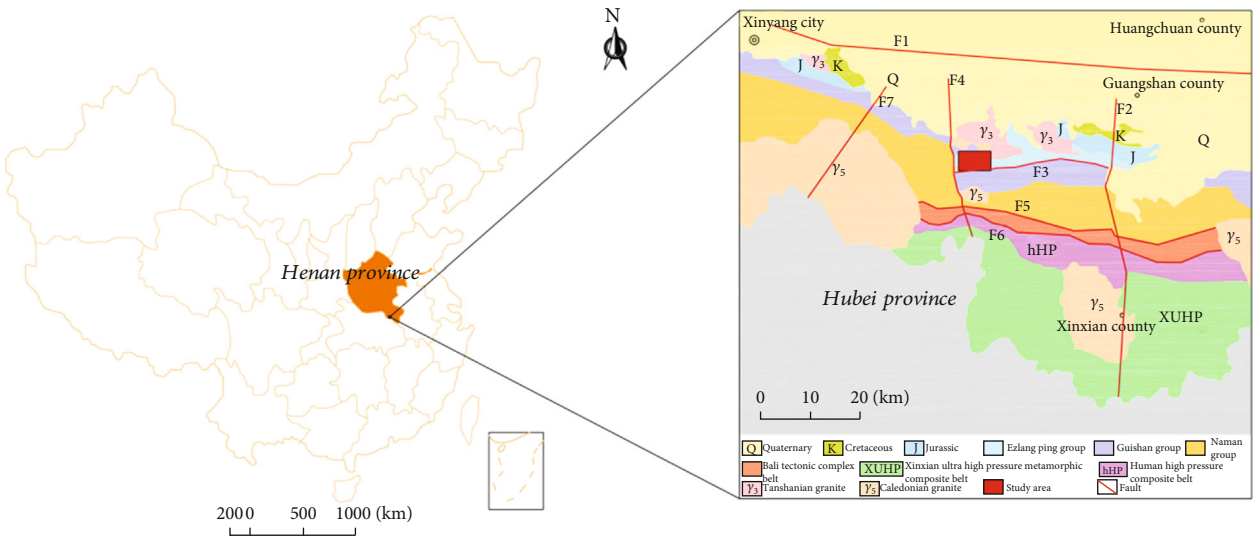

Figure 1: The study area location.

Figure 2: The selected instruments.

the unit was used to determine the permeability of the rock close to the borehole. The length of the test section is chosen for rock sections with high permeability, such as tectonic fracture zones and fracture development zones, based on particular circumstances. In order to ensure that no test section was missed, a tiny amount of overlap between neighboring test sections was permitted. The remaining core was then used to calculate the test length.

2.3. Correlation of Permeability and Electrical Resistivity

2.3.1. Permeability and Electrical Resistivity Characteristics with Depth. After drilling, water is injected into the borehole until the water level is roughly level with the top of the borehole. Then, using apparent resistivity logging in geophysical logging technology, the apparent resistivity data of the rock surrounding the borehole are obtained from top to bottom

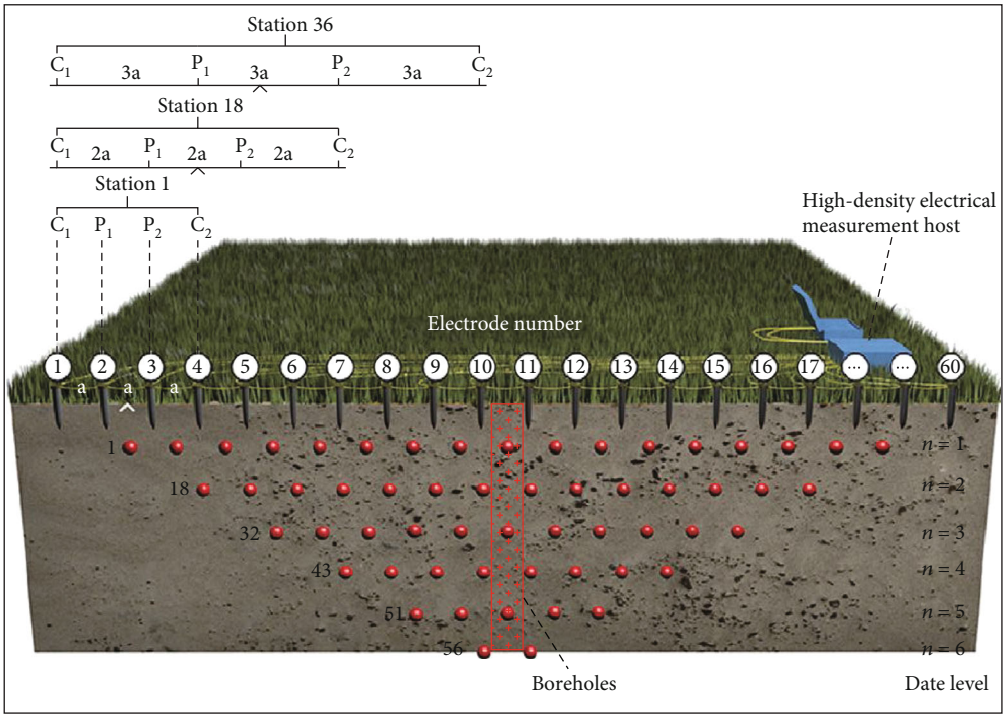

Figure 3: The distribution diagram of Wenner-Alpha method.

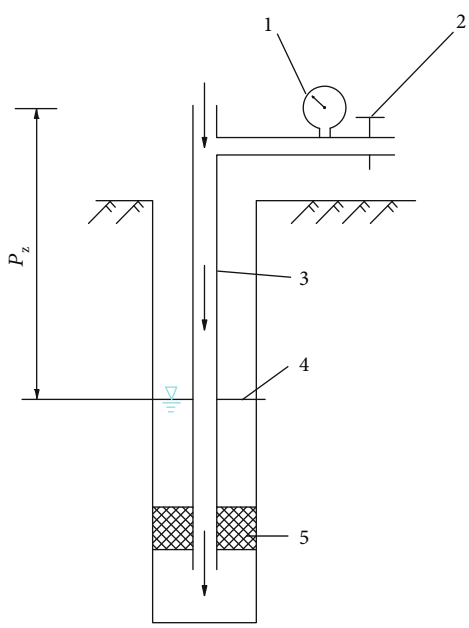

1-Pressure Gauge; 2-Water Inlet Valve; 3-Water Inlet Pipe; 4-Groundwater Level; 5-Trial embolization; Pz-Water Column Pressure (MPa)

Figure 4: Schematic representation of the water pressure test.

at a spacing of 1 m. The effectiveness and feasibility of the models in this rock mass were compared and examined with the actual geological survey data based on the electrical resistivity and Lugeon value data at different depths. Figures 6 and 7 depict the electrical resistivity and Lugeon value curves of the two boreholes.

2.3.2. Model of Electrical Resistivity and Lugeon Value. Three different common models, including the power function, exponential function, and polynomial function models, were used to ascertain the quantitative relationship between electrical resistivity and Lugeon value in order to further examine this relationship. The electrical resistivity and Lugeon value of borehole 1 were fitted using the least squares approach to provide the equations of each model and the correlation coefficients, as shown in Table 1 and Figure 8.

Table 1 shows that there are some differences in the correlation between the three models, and while the polynomial model is the best option, it is still insufficient for this study.

2.3.3. Model Selection. The polynomial and exponential models are thought to be superior to the power function model based on error and correlation coefficient analysis, but in order to compare how well each model applies in practice, the permeability zoning at the borehole is inverted using surfer software, which can see the permeability distribution at the borehole and perform an analytical comparison. Borehole 1 was chosen for the analysis, and Figure 9 displays the fit of each function model.

The applicability of the model is further analyzed from Figure 9.

(1) Assume that the relationship between electrical resistivity and Lugeon value is a power function. Then, using the fitted relation $q = 119883\,\Omega^{-1.78}$ and the measured electrical resistivity, get the calibration permeability coefficient and create a graph using the surfer software. The calibrated permeability found in Figure 9(a), which was produced by inverting the power function model, is within

Figure 5: The water pressure test.

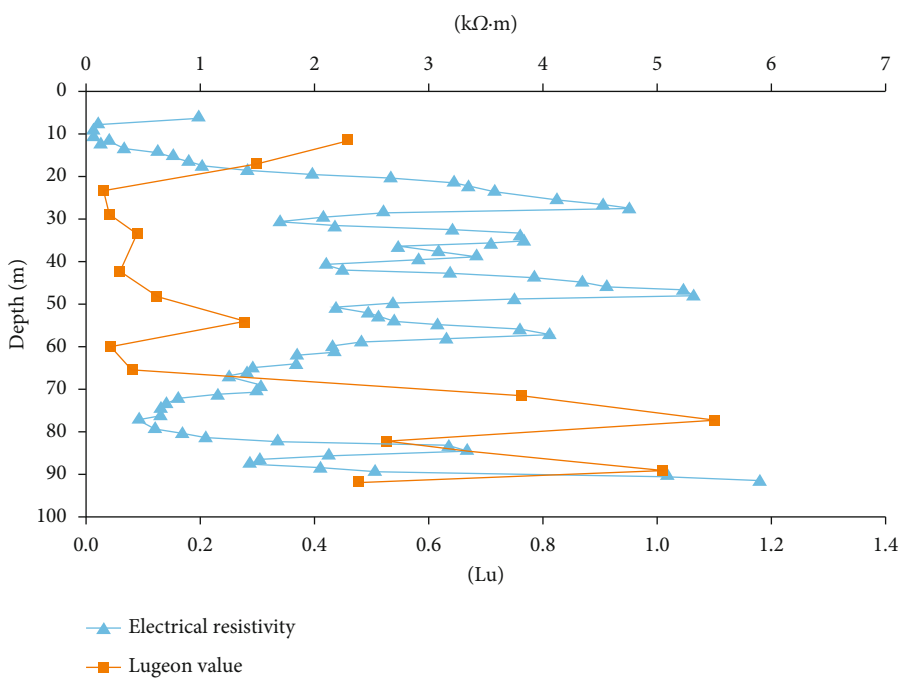

Figure 6: Borehole 1 comparison curves of electrical resistivity and Lugeon value results.

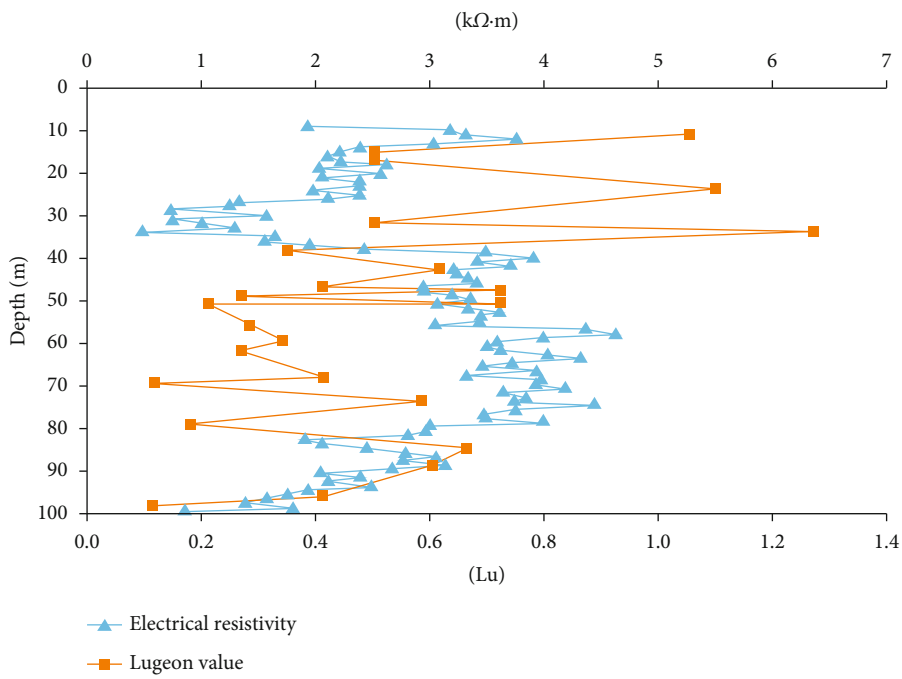

Figure 7: Borehole 2 comparison curves of electrical resistivity and Lugeon value results.

Table 1: Model analysis table of the relationship between electrical resistivity and Lugeon value.

Mathematical models	Fitted model equation	Correlation efficient
Power function	$q = 119883\,\Omega^{-1.78}$	0.865
Exponential function	$q = 1.85e^{-0.0001\Omega}$	0.789
Polynomial function	$q = 1 \times 10^{-7}\,\Omega^2 - 0.0008\,\Omega + 1.4165$	0.884

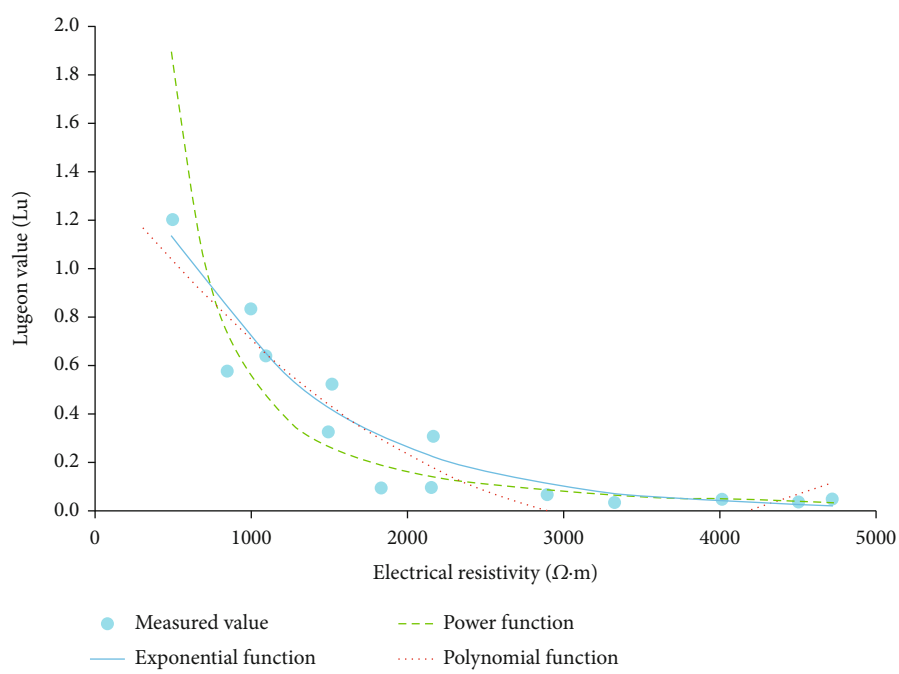

Figure 8: Borehole 1 model diagram of the relationship between electrical resistivity and Lugeon value.

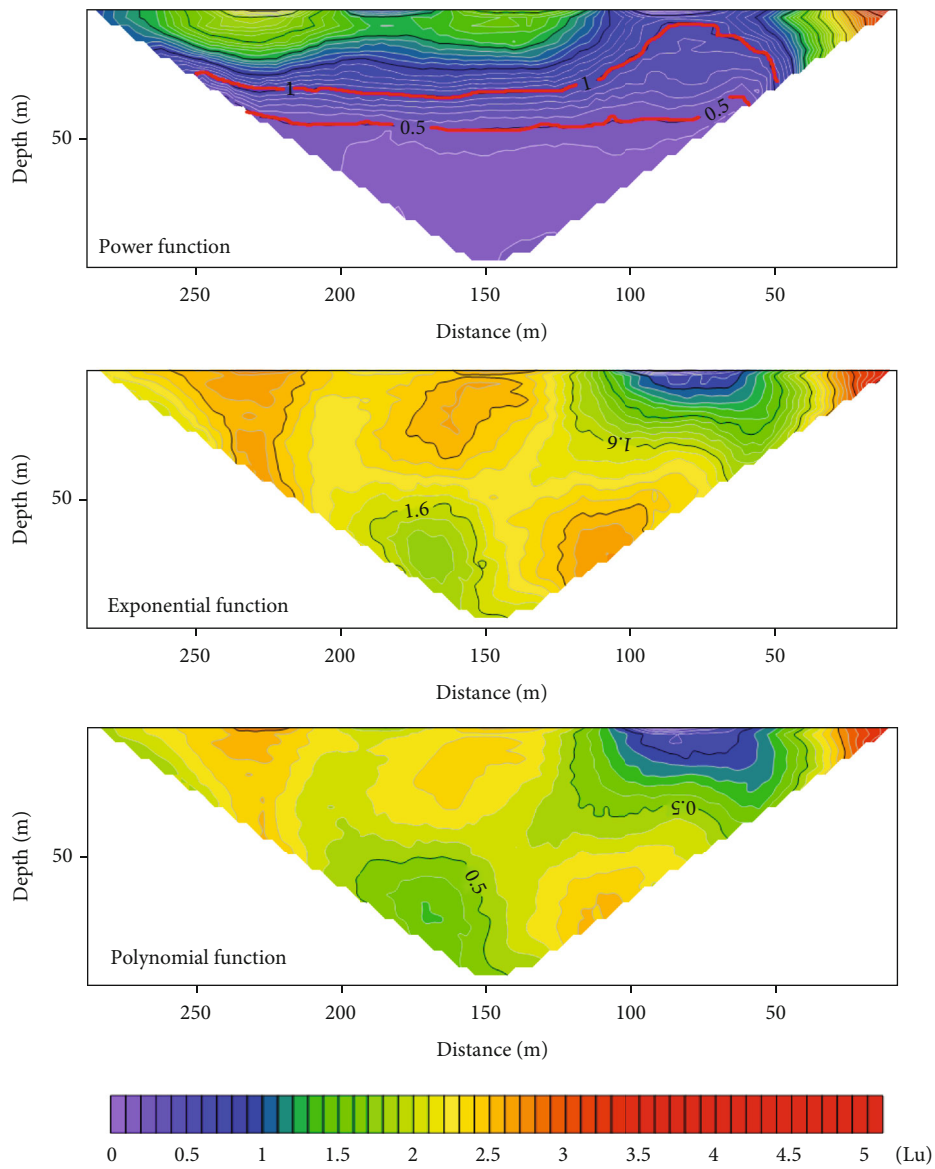

Figure 9: The fit of each function model.

the range of normal values and has a wide range of applications

(2) The relationship between electrical resistivity and Lugeon value is considered to be an exponential function, and the fitted relationship $q = 1.85e^{-0.0001\Omega}$ is used to generate a graph using the software surfer (see Figure 9(b)). Although they are within the usual range, the figure with the exponential function model inversion of the calibrated permeability shows that, despite the inaccuracy of the power function being quite significant, the applicability is not excessively wide

(3) Assume that there is a polynomial relationship between electrical resistivity and Lugeon value, and then, use the fitted relationship, $q = 1 \times 10^{-7}\,\Omega^2 - 0.0008\,\Omega + 1.4165$, to create a graph (see Figure 9(c)). The graph demonstrates that the calibrated permeability, which was produced by inversion with the exponential function model, has a partially negative value, which is anomalous and inconsistent with reality

In an effort to establish the electrical resistivity and Lugeon value, the one-to-one correlation between electrical resistivity and Lugeon value was utilized to extract data in the previous phase. And power function, exponential, polynomial, and other fitting formulas were chosen for error analysis comparison of experimental data. And it was concluded that the power function model was a better appropriate model parameter for their interaction. As demonstrated in Figure 9(a) and the equation for the calibration curve,

$$q = 119883\Omega^{-1.78} R2 = 0.865, \quad (1)$$

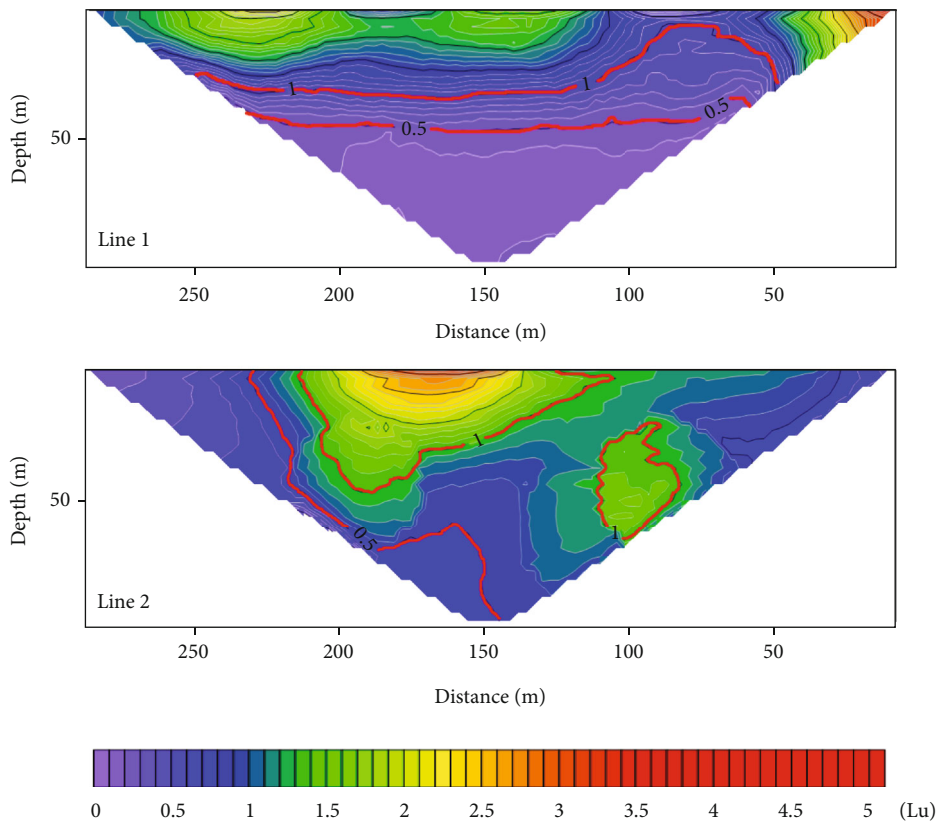

Figure 10: The permeability zoning map.

where q is media permeability (Lu), Ω is media resistivity (Ω•m), and R^2 is correlation coefficient; the absolute value of correlation coefficient below 0.3 is no linear correlation, above 0.3 is linear correlation, 0.3 to 0.5 is low correlation, and 0.5 to 0.8 is a significant correlation (moderate correlation), and above 0.8 is a high correlation.

The fitted formula has a correlation coefficient of 0.866, which is a very high correlation and preliminary evidence that the power function connection model is more suitable.

3. Electrical Resistivity Inversion of Rock Permeability Zoning

The ring reservoir watershed was divided in the profile using the ERT profile in accordance with the equation (1) that describes the link between electrical resistivity and Lugeon value. The ring reservoir was separated vertically into three zones based on the permeability calculated from conductivity: very slightly permeable zone ($q < 0.1$ Lu), slightly permeable zone ($0.1\ \text{Lu} \le q < 1\ \text{Lu}$), and weakly permeable zone ($1\ \text{Lu} \le q < 10\ \text{Lu}$). The results of the permeability zone of the rock next to the borehole, as determined by the water pressure test, are as follows.

Very slightly permeable zone: the permeability q is less than 0.1 Lu and is primarily dispersed in borehole 1, which comprises 11.6% of the entire test section

Micropermeability zone: permeability q, dispersed in both boreholes and making up 62.8% of the entire test section, is between 0.1 Lu and 1.0 Lu

Weakly permeable zone: the permeability q, which makes up 25.6% of the entire test section, is distributed among both boreholes and ranges from 1.0 Lu to 10.0 Lu

Figure 10 analyzes the permeability properties of the rocks close to boreholes 1 and 2. It demonstrates that the 0.5 Lu line (red mark) is essentially consistent with the findings of the previous drilling and has some guiding significance for the permeability zoning of the upper reservoir ring profile in the study area. To serve as a guide for the construction of the reservoir's perimeter impermeability, the 0.5 Lu and 1.0 Lu lines are employed as the distinctive dividing lines in the figure.

4. Conclusion

Taking a pumped storage power station as an example, this study obtained the following results by analyzing the relationship between the permeability and electrical resistivity of granite mass.

(1) In order to assure the accuracy of the findings of the calculation for rock permeability, it is necessary to install a particular check valve to the pressure gauge's inlet during water pressure testing. This may effectively prevent the mechanical mistake produced by pressure instability on the reading

(2) All three models—power function, exponential function, and polynomial function—showed good applicability when the electrical resistivity and Lugeon

value of the borehole were fitted using the least squares method, with the polynomial model performing the best. However, the split displayed negative values, which did not correspond to the reality. The calibrated permeability resulting from the inversion of the power function model has the best application in a thorough study

(3) The permeability partitioning of the two ERT lines by the power function relationship model may more clearly produce the characteristic partition lines of 0.5 Lu and 1.0 Lu, indicating that this method has some relevance and can serve as a guide for the design of reservoir impermeability

As far as geology is concerned, the geological environment is different in different regions. For hydropower projects that concern people's livelihood, a combination of multiple methods should be used and complement each other according to the different characteristics of the study area in order to have a more in-depth and accurate understanding of the study area.

Data Availability

All data, models, and code generated or used during the study appear in the submitted article.

Conflicts of Interest

The authors declare that they have no conflicts of interest.

Acknowledgments

This study was supported by the Central Plains Science and Technology Innovation Leader Project (214200510030), Key Scientific Research Project of Colleges and Universities in Henan Province (20A410001), and Key Research and Development Project of Henan Province (221111321500).

References

[1] Ministry of Water Resources of the People's Republic of China, *National Statistical Bulletin on Water Resources Development in 2018*, China Water Conservancy and Hydropower Press, 2019.

[2] R. X. Jin, "Study on the permeability stability of a reservoir dam base," *Rock and Soil Mechanics*, vol. 25, no. 1, pp. 157–159, 2004.

[3] J. H. Yao, S. J. Luo, and W. J. Song, "Application of integrated physical prospecting in reservoir leakage detection," *Physical and Chemical Exploration*, vol. 44, no. 2, pp. 456–462, 2020.

[4] D. Yuan and Q. H. Zhang, "Calculation method of permeability coefficient of homogeneous aquifer based on piezometric test," *Journal of the Changjiang Academy of Sciences*, vol. 31, no. 8, pp. 77–81, 2014.

[5] G. E. Archie, "The electrical resistivity log as an aid in determining some reservoir characteristics," *Transactions of the AIME*, vol. 146, no. 1, pp. 54–62, 1942.

[6] R. G. Campanella and I. Weemee, "Development and use of an electrical resistivity cone for groundwater contamination studies," *Canadian Geotechnical Journal*, vol. 27, no. 5, pp. 557–567, 1990.

[7] Y. Wang, Z. Y. Song, T. Q. Mao, and C. Zhu, "Macro-meso fracture and instability behaviors of hollow-cylinder granite containing fissures subjected to freeze-thaw-fatigue loads," *Rock Mechanics and Rock Engineering*, vol. 55, no. 7, pp. 4051–4071, 2022.

[8] L. H. Han, S. Y. Liu, and Y. J. Du, "A new method for detecting contaminated soil-resistivity method," *Chinese Journal of Geotechnical Engineering*, vol. 28, no. 8, pp. 1028–1032, 2006.

[9] X. C. Chen, Y. Song, X. J. Chen, P. Y. Bi, X. Huang, and D. X. Liang, "Experimental study on resistivity characteristics of Cu^{2+} contaminated red clay," *Rock and Soil Mechanics*, vol. 41, no. S2, pp. 1–10, 2020.

[10] Y. Wang, J. Z. Li, C. Zhu, and T. Mao, "Fatigue failure identification using deformation and energy rate for hole-fissure contained granite under freeze-thaw and variable-frequency-variable-amplitude cyclic loads," *Fatigue & Fracture of Engineering Materials & Structures*, vol. 45, no. 3, pp. 834–851, 2022.

[11] G. H. Liu, Z. Y. Wang, and J. P. Huang, "Resistivity properties of soils and their engineering applications," *Chinese Journal of Geotechnical Engineering*, vol. 26, no. 1, pp. 83–87, 2004.

[12] F. S. Zha, S. Y. Liu, Y. J. Du, and K. R. Cui, "Resistivitybased suction prediction of unsaturated soil matrix," *Geotechnics*, vol. 31, no. 3, pp. 1003–1008, 2010.

[13] L. H. Zhang, B. Z. Pan, Z. B. Li, X. W. Mo, Z. L. Xia, and W. L. Xu, "New three-water conductivity model and its application in the evaluation of low-hole and low-permeability reservoirs," *Chinese Petroleum Geophysical Exploration*, vol. 45, no. 3, pp. 431–435, 2010.

[14] Y. Wang, T. Mao, Y. Xia, X. Li, and X. Yi, "Macro-meso fatigue failure of bimrocks with various block content subjected to multistage fatigue triaxial loads," *International Journal of Fatigue*, vol. 163, article 107014, 2022.

[15] L. H. Han, S. Y. Liu, and Y. J. Du, "Experimental study on the effect of temperature on the resistivity of contaminated soil," *Rock and Soil Mechanics*, vol. 28, no. 6, pp. 1151–1155, 2007.

[16] W. X. Sima, L. Luo, T. Yuan, Q. Yang, C. P. Lei, and C. L. Jiang, "Temperature characteristics of soil resistivity and its influence on the heating of DC grounding electrode," *High Voltage Technology*, vol. 38, no. 5, pp. 1192–1198, 2012.

[17] Y. Wang, J. Han, Y. Xia, and D. Long, "New insights into the fracture evolution and instability warning predication for fissure-contained hollow-cylinder granite with different hole diameter under multi-stage cyclic loads," *Theoretical and Applied Fracture Mechanics*, vol. 119, article 103363, 2022.

[18] C. Clavier, G. Coates, and J. Dumanoir, "Theoretical and experimental bases for the dual-water model for interpretation of shaly sands," *Society of Petroleum Engineers Journal*, vol. 24, no. 2, pp. 153–168, 1984.

[19] Q. C. Xue, "Preliminary results on the estimation of hydrogeological parameters in the Chengdu plain using electrical bathymetry data," *Geophysical and Geochemical Exploration*, vol. 11, no. 5, pp. 396–399, 1987.

[20] X. Y. Yu and J. P. Xia, "Application of electric bathymetry results to calculate hydrogeological parameters," *Carsologica Sinica*, vol. 8, no. 4, pp. 73–78, 1989.

[21] Y. C. Yu and J. C. Wu, "A preliminary study on the use of ERT data to derive permeability coefficients of non-homogeneous

porous media," *Chinese Hydrogeology and Engineering Geology*, no. 2, pp. 41–44, 2006.

[22] A. T. Tizro, K. S. Voudouris, M. Salehzade, and H. Mashayekhi, "Hydrogeological framework and estimation of aquifer hydraulic parameters using geoelectrical data: a case study from West Iran," *Hydrogeology Journal*, vol. 18, no. 4, pp. 917–929, 2010.

[23] S. Perdomo, J. E. Ainchil, and E. Kruse, "Hydraulic parameters estimation from well logging resistivity and geoelectrical measurements," *Journal of Applied Geophysics*, vol. 105, no. 2, pp. 50–58, 2014.

[24] Energy Bureau of the People's Republic of China, *Regulations for Piezometric Testing of Boreholes in Hydropower Projects*, China Water Conservancy and Hydropower Press, 2018.

[25] K. K. Xu, "Comparative analysis of domestic regulations and international standards for water pressure testing of hydropower and water conservancy projects," *Chinese Survey Science and Technology*, no. 4, pp. 7–13, 2019.